



Rock Physical Modeling and Seismic Dispersion Attribute Inversion for the Characterization of a Tight Gas Sandstone Reservoir

Han Jin¹, Cai Liu¹, Zhiqi Guo^{1*}, Yiming Zhang², Cong Niu², Di Wang² and Yun Ling²

¹ College of Geo-Exploration Science and Technology, Jilin University, Changchun, China, ² CNOOC Research Institute Co., Ltd., Beijing, China

OPEN ACCESS

Edited by:

Jing Ba,
Hohai University, China

Reviewed by:

Zhiwei Wang,
China University of Petroleum
(Huadong), China
Fei Gong,
China University of Petroleum, China

*Correspondence:

Zhiqi Guo
zhiqigu@aliyun.com

Specialty section:

This article was submitted to
Solid Earth Geophysics,
a section of the journal
Frontiers in Earth Science

Received: 14 December 2020

Accepted: 01 March 2021

Published: 29 April 2021

Citation:

Jin H, Liu C, Guo Z, Zhang Y,
Niu C, Wang D and Ling Y (2021)
Rock Physical Modeling and Seismic
Dispersion Attribute Inversion
for the Characterization of a Tight Gas
Sandstone Reservoir.
Front. Earth Sci. 9:641651.
doi: 10.3389/feart.2021.641651

Gas identification using seismic data is challenging for tight gas reservoirs with low porosity and permeability due to the complicated poroelastic behaviors of tight sandstone. In this study, the Chapman theory was used to simulate the dispersion and attenuation caused by the squirt flow of fluids in the complex pore spaces, which are assumed to consist of high aspect-ratio pores (stiff pores) and low aspect-ratio microcracks (soft pores). The rock physics modeling revealed that as the gas saturation varies, P-wave velocity dispersion and attenuation occurs at seismic frequencies, and it tends to move to high frequencies as the gas saturation increases. The velocity dispersion of the tight gas sandstone causes a frequency-dependent contrast in the P-wave impedance between the tight sandstone and the overlying mudstone, which consequently leads to frequency-dependent incidence reflection coefficients across the interface. In the synthetic seismic AVO modeling conducted by integrating the rock physics model and the propagator matrix method, the variations in the amplitudes and phases of the PP reflections can be observed for various gas saturations. The tests of the frequency-dependent AVO inversion of these synthetic data revealed that the magnitude of the inverted P-wave dispersion attribute can be used to indicate gas saturation in tight sandstone reservoirs. The applications of the frequency-dependent AVO inversion to the field pre-stacked seismic data revealed that the obtained P-wave dispersion attribute is positively correlated with the gas production from the pay zone at the well locations. Thus, the methods of the rock physics modeling and the frequency-dependent AVO inversion conducted in this study have good potential for the evaluation of the gas saturation in tight gas sandstone reservoirs.

Keywords: tight gas sandstone, rock physics, seismic responses, dispersion attribute, gas saturation

INTRODUCTION

Tight gas sandstone is generally characterized by a strong heterogeneity, low effective porosity, and extremely low permeability. It is challenging to predict the complicated poroelastic behaviors of tight gas sandstone due to the presence of a complex pore and crack system. Correspondingly, the seismic responses from tight gas sandstone are complex because of the dispersion and attenuation caused by the squirt flow of fluids in the complex pore spaces when the seismic waves pass through the tight sandstone. Thus, in order to evaluate the fluid properties of tight sandstone, it is essential to construct valid rock physics models for the investigation

of seismic dispersion and attenuation and to develop effective techniques for estimating gas saturation using such poroelastic properties.

For rock physics modeling for a poroelastic medium, Biot (1956a,b) established a macroscopic pore elasticity model in order to consider global fluid-flow in a fluid saturated medium. White (1975) proposed a model that considers the dispersion and attenuation that occurs at the seismic frequencies associated with the patchy saturation of two fluid phases. Dvorkin and Nur (1993) developed the Biot/Squirt (BISQ) model by combining the global Biot flow and the local squirt-flow mechanism. Chapman et al. (2002) and Chapman (2003, 2009) proposed the theory of multiscale fractures for an effective medium containing microscopic pores and cracks and with mesoscopic fractures. Ba et al. (2012) investigated the Biot-Rayleigh theory for modeling tight gas sandstone using a double-pore model. Ba et al. (2016) researched compressional wave dispersion due to rock matrix stiffening by clay squirt flow. Ba et al. (2017) investigated the wave propagating in an anelastic rock with patchy-saturation and fabric heterogeneity.

For the investigation of the seismic responses associated with fluid flow, the frequency-dependent amplitude variation with offset (AVO) method was proposed. Chapman et al. (2005, 2006) analyzed the frequency dependency of the AVO signatures associated with the dispersion and attenuation caused by the presence of fluids. Wilson et al. (2009) and Wilson (2010) extended the conventional AVO approximation to frequency dependency and derived the P-wave dispersion attribute as an indicator for reservoir fluid characterization, in which the spectral decomposition technique was used in the implement of the dispersion attribute inversion. Wu (2010) improved the accuracy of the time-frequency analysis in the inversion in the application of field data. Zhang et al. (2014) extended the AVO Shuey approximation and introduced the concepts of a frequency-dependent intercept and gradient into the AVO inversion. Li (2013) investigated numerical and physical modeling as well as field data for the frequency-dependent AVO in order to enable the quantitative estimation of gas saturation. Wu et al. (2014) also illustrated another field case study of the frequency-dependent AVO by improving the procedure of inversion. Chen et al. (2015) quantitatively calculated the gas saturation based on the dispersion inversion using stacked seismic data. Wang et al. (2019) investigated the problem of reflection and transmission of plane elastic waves at an interface between two double-porosity media.

In this study, we developed a rock physics model for a tight gas sandstone reservoir based on the Chapman theory that considers the squirt flow of fluids in complex pore spaces. Then we used our model to investigate the influence of gas saturation on P-wave velocity dispersion and attenuation. The frequency-dependent AVO modeling and inversion were tested and analyzed for various gas saturations using synthetic data. Finally, the frequency-dependent AVO inversion was applied to field data for a tight gas sandstone reservoir, and the P-wave dispersion attributes were inverted and calibrated in order to determine the gas saturation in the tight sandstone reservoir.

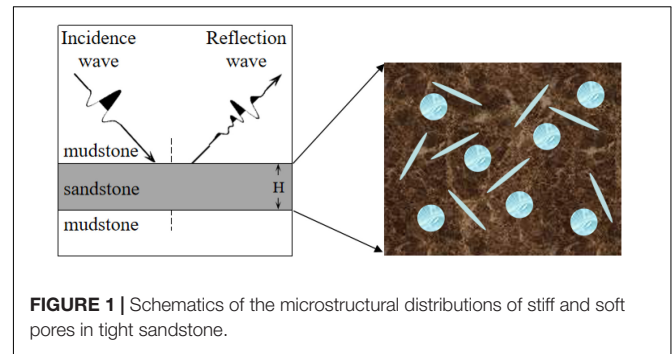


FIGURE 1 | Schematics of the microstructural distributions of stiff and soft pores in tight sandstone.

MATERIALS AND METHODS

Rock Physics Model of Tight Sandstone

For tight gas sandstone reservoirs, their complex pore structures result in complicated elastic properties and seismic responses associated with fluids. Smith et al. (2009) and Ruiz and Cheng (2010) investigated a rock model including soft and stiff pores, which divided the complex pores into stiff pores and soft pores. They studied the influence of the distributions of stiff and soft pores on the elastic properties of tight sandstone. Their results indicated that the dual-porosity model can well predict the elastic behaviors of tight sandstone. However, this model could not describe inelasticity associated with fluids. Chapman (2003) proposed the theory of multiscale pores and fractures and studied the dispersion and attenuation related to the squirt flow of fluids in complex pore spaces in gas sandstone reservoirs. Thus, we used the concept of stiff and soft pores in Chapman's theory to describe pore structures of tight gas sandstone reservoirs. A schematic diagram of the complex pore spaces consisting of stiff and soft pores is shown in **Figure 1**.

In Chapman's theory (Chapman, 2003), the expression for the anisotropic stiffness matrix of an equivalent medium is

$$C_{ijkl} = C_{ijkl}^0 - \phi_p C_{ijkl}^1 - \epsilon_c C_{ijkl}^2 - \epsilon_f C_{ijkl}^3 \quad (1)$$

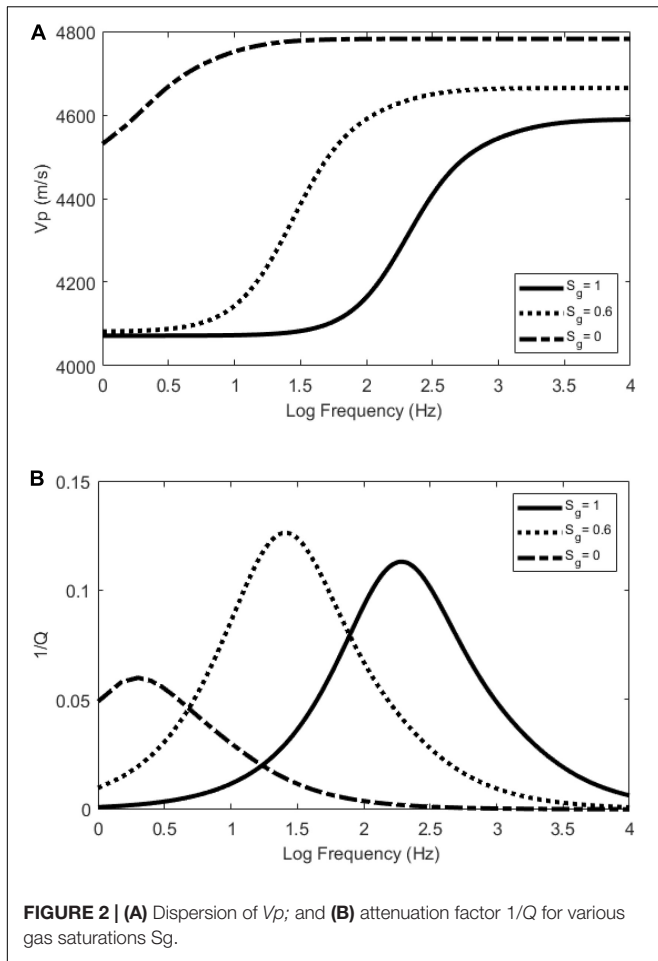
where C_{ijkl}^0 is the stiffness of the isotropic background; C_{ijkl}^1 , C_{ijkl}^2 , and C_{ijkl}^3 are the disturbances caused by the pores, micro-cracks, and fractures, respectively; ϕ_p is the porosity; ϵ_c is the crack density; and ϵ_f is the fracture density.

According to geological understanding of the tight sandstone reservoir in this study area, mesoscale fractures are not developed, and the pore space is dominated by micro pores and cracks. Thus, in Eq. 1, we maintain the terms of the micro pores and cracks, while we drop the term of the mesoscale fractures. So, Eq. 1 becomes

$$C_{ijkl} = C_{ijkl}^0 - \phi_p C_{ijkl}^1 - \epsilon_c C_{ijkl}^2 \quad (2)$$

According to Chapman et al. (2002), the relaxation time τ plays an important role in determining the frequency bandwidth of the seismic dispersion and attenuation:

$$\tau = \frac{4\eta a^3 (1 - \nu)}{9k_s \zeta \mu} \quad (3)$$



where μ is the shear modulus; and ν is the Poisson ratio of the solid matrix. a is the crack radius; r is the aspect ratio; η is the fluid viscosity; ζ is the grain size; and k is the permeability.

The frequency-dependent P-wave velocity $V_p(\omega)$ and the attenuation factor $1/Q(\omega)$ can be calculated from $C_{3333}(\omega)$ in Eq. 2 and the density ρ_s of the fluid-saturated sandstone. The equations are as follows:

$$V_p(\omega) = \sqrt{\frac{C_{3333}(\omega)}{\rho_s}} \tag{4}$$

$$\frac{1}{Q(\omega)} = \frac{\text{Im}(C_{3333}(\omega))}{\text{Re}(C_{3333}(\omega))} \tag{5}$$

where Re and Im indicate the real part and imaginary part of a complex modulus, respectively.

Physical Parameters of a Mixed Fluid

The viscosity of the mixed fluid in Eq. 1 has an impact on the frequency band of the dispersion and attenuation. For a mixture of water and gas, the viscosity has the following form (Davide and Carcione, 2003):

$$\eta = \eta_g \left(\frac{\eta_w}{\eta_g} \right)^{1-S_g} \tag{6}$$

TABLE 1 | Properties of tight gas sandstone.

Property	Symbol	Value	Unit
P velocity	V_p	4,500	m/s
S velocity	V_s	2,500	m/s
Sandstone density	ρ	2,460	kg/m ³
Water velocity	V_w	1,710	m/s
Gas velocity	V_g	620	m/s
Water density	ρ_w	1,000	kg/m ³
Gas density	ρ_g	65	kg/m ³
Water viscosity	η_w	2×10^{-5}	Pa·s
Gas viscosity	η_g	3×10^{-3}	Pa·s
Porosity	φ_p	0.1	
Crack density	ϵ_c	0.1	
Permeability	K	0.1	mD
Aspect ratio	r	2×10^{-4}	
Crack/pore radius	a	2×10^{-4}	m
Grain size	ζ	2×10^{-4}	m
Poisson ratio	σ	0.25	
Shear modulus	μ	21	GPa

where η_g is the viscosity of the gas; η_w is the viscosity of water; and S_g is the gas saturation.

Under different gas saturations, the density of the fluid mixture and that of the fluid saturated sandstone are as follows:

$$\rho_f = S_g \rho_g + (1 - S_g) \rho_w \tag{7}$$

$$\rho_s = \varphi \rho_f + (1 - \varphi) \rho_m. \tag{8}$$

where ρ_f is the density of the fluid mixture; ρ_g is the density of the gas; ρ_w is the density of water; ρ_s is the density of the saturated rock; ρ_m is the density of the solid matrix; and φ is the porosity.

The bulk module K_f and the velocity V_f of the fluid mixture are calculated using Wood's equations (Wood, 1995):

$$K_f = \frac{1}{\frac{S_g}{K_g} + \frac{1-S_g}{K_w}} \tag{9}$$

$$V_f = \sqrt{\frac{K_f}{\rho_f}} \tag{10}$$

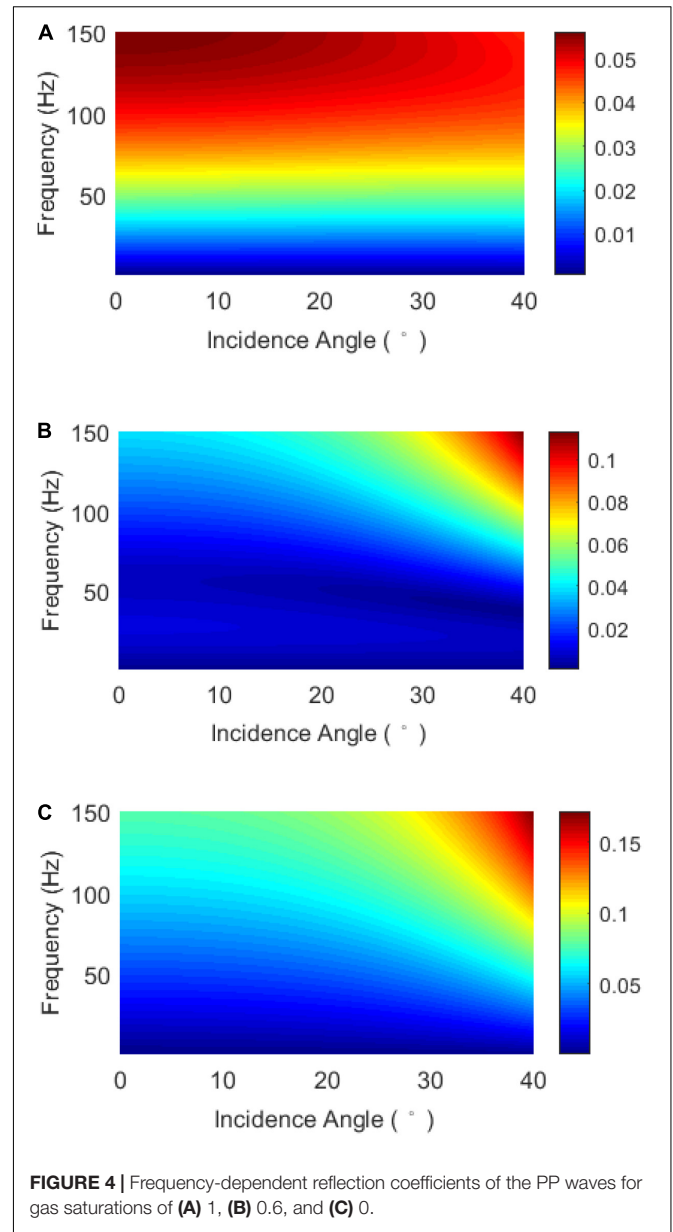
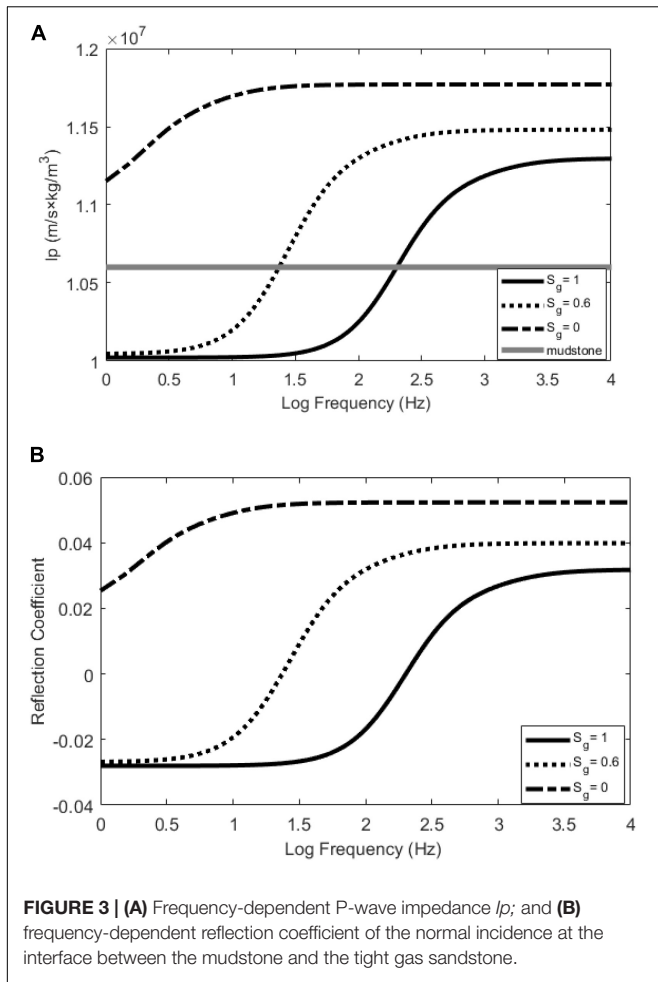
In these equations, K_g and K_w are the bulk modulus of gas and water, respectively.

The Method for the Modeling of the Frequency-Dependent AVO

Based on the rock physics model, the propagator matrix theory was used to calculate the seismic responses of the tight sandstone gas reservoir.

The reflection and transmission coefficient vectors $r = [R_{PP}, R_{PS}, T_{PP}, T_{PS}]$ in the case of the P-wave incidence are solved using the following equation (Carcione, 2001):

$$r = - \left[A_1 - \left(\prod_{\alpha=1}^N B_\alpha \right) A_2 \right]^{-1} i_p \tag{11}$$



where the matrices A_1 and A_2 are the propagation matrices related to the elastic moduli of the upper and lower media, respectively. $B_{\alpha}=T(0)T^{-1}(h_{\alpha})(\alpha=1,\dots,N)$ is the propagation matrix of the middle layer, which has an N-layer structure. h_{α} is the thickness of each individual layer. i_p is the P-wave incident vector related to the elastic properties of the incidence medium.

The reflection coefficient R_{pp} at each frequency can be calculated using the propagator matrix theory. We use R_f to denote R_{pp} in the following. By multiplying the frequency reflection coefficient R_f by the spectrum of the seismic wavelet W_f , we can calculate the amplitude spectrum U_f of the reflected wave.

$$U_f = W_f \times R_f \tag{12}$$

After the inverse Fourier transform of U_f , the reflection waveform U_t in the time domain can be calculated as

$$U_t = \frac{1}{2\pi} \int_{-\infty}^{\infty} U_f \exp(-i2\pi ft) df \tag{13}$$

where f is the angular frequency; i is the unit of the imaginary number; and t is time.

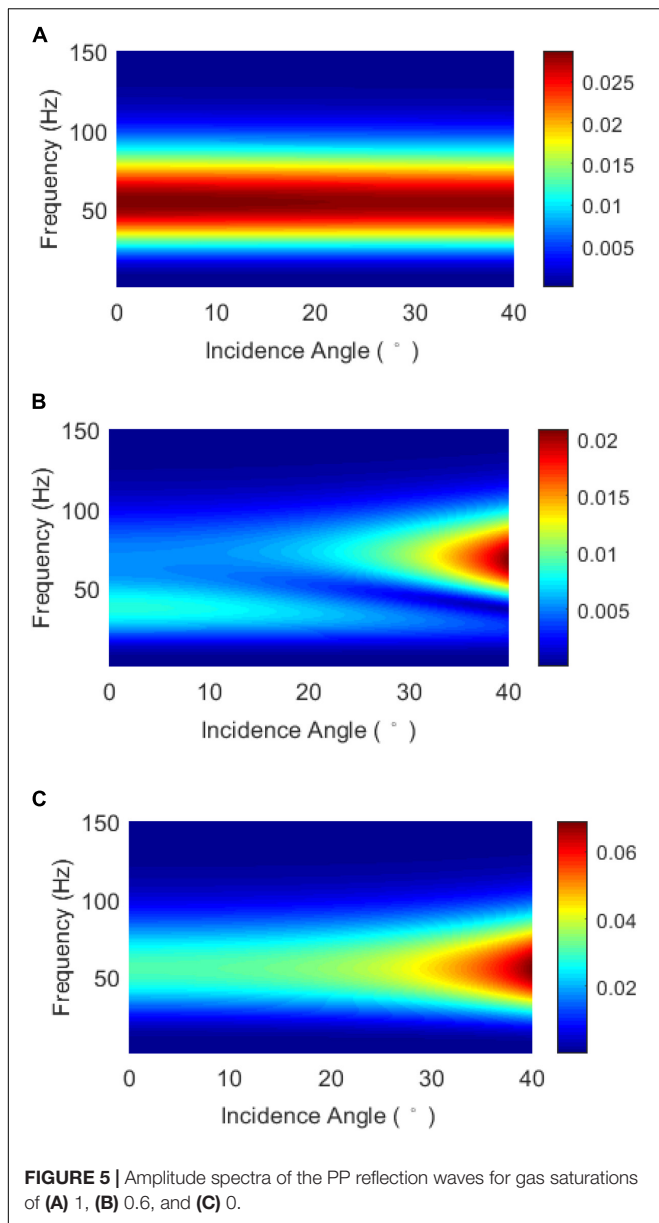
The Frequency-Dependent AVO Theory

Based on the AVO approximate formula given by Shuey (1985); Chapman et al. (2006) deduced the frequency-dependent AVO formula shown as

$$R_{pp}(\theta, f) = R_{pp}(\theta, f_0) + D_P(f - f_0) + D_G(f - f_0) \sin^2 \theta \tag{14}$$

where D_P represents the derivatives of the seismic wave velocities with frequency; and D_G is the frequency-dependent AVO gradient.

$$D_P = \frac{\partial}{\partial f} \left(\frac{\Delta V_P(f)}{2V_P(f)} \right), \text{ and } D_G = \frac{\partial G(f)}{\partial f} \tag{15}$$

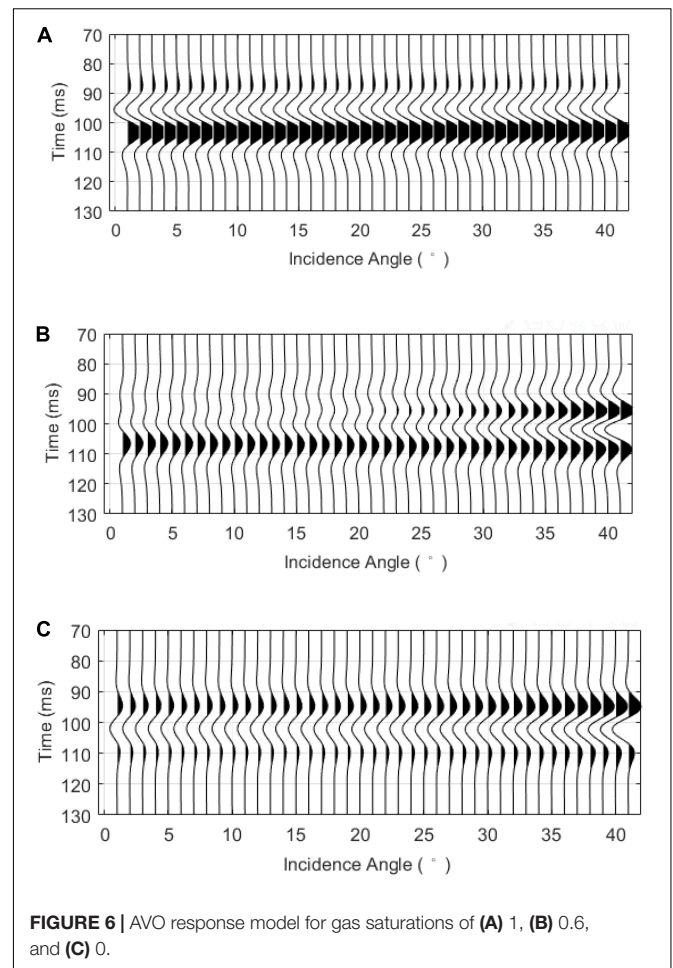


Equations 14, 15 form the basis of the frequency-dependent AVO inversion. More details for the implementation of the inversion are displayed in **Appendix A**.

MODELING AND INVERSION USING SYNTHETIC DATA

Dispersion and Attenuation in Tight Sandstone

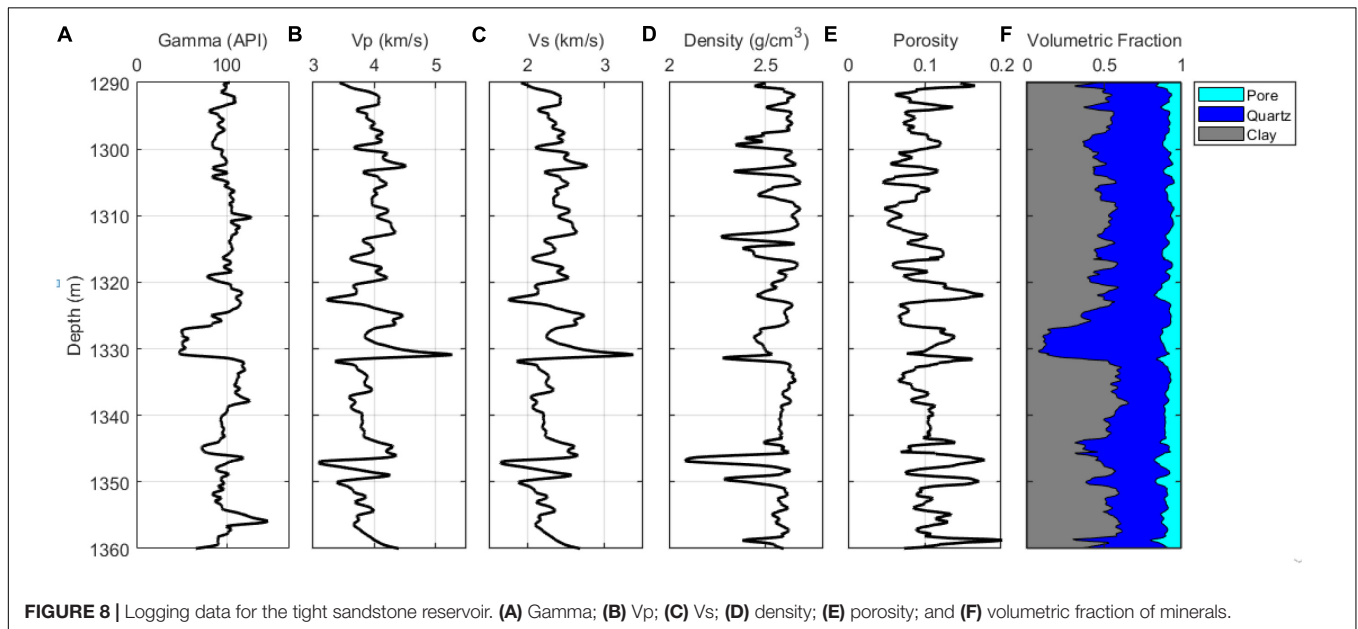
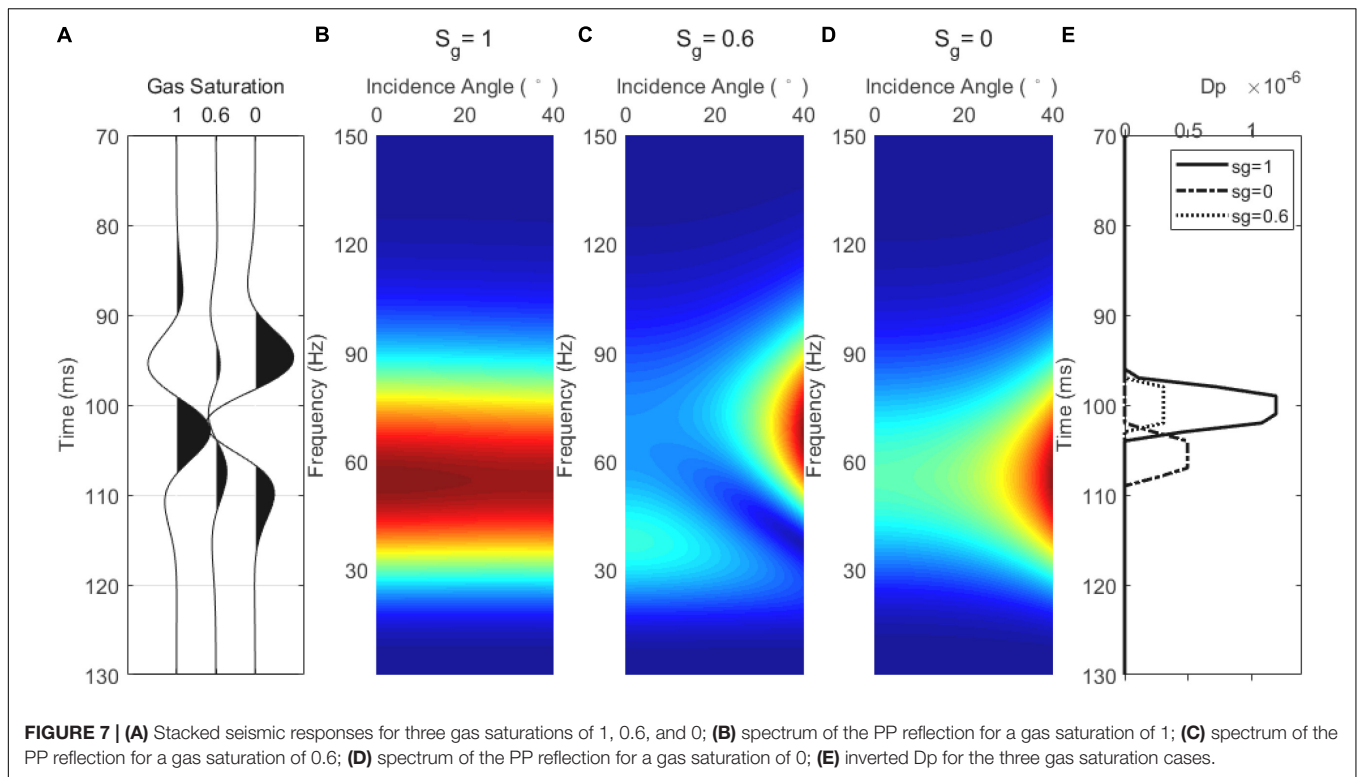
Based on the rock physics model discussed above, **Figure 2** shows the calculated velocity dispersion and attenuation of a tight gas sandstone reservoir for different gas saturations. The properties used in the rock physics model are presented in **Table 1**. As can be seen from **Figure 2A**, the P-wave velocity V_p in the



seismic frequency bandwidth decreases as the gas saturation S_g increases from 0 to 0.6 to 1. Moreover, the range of the frequency at which the velocity dispersion occurs moves to a higher frequency. Accordingly, as illustrated in **Figure 2B**, the attenuation peak also moves to a higher frequency as S_g increases. According to Eqs. 3, 6, S_g affects the viscosity coefficient of the fluid mixture, and thus, it changes the relaxation time parameter τ , which controls the frequency range of the velocity dispersion and attenuation. Therefore, variations in the gas saturation have a significant impact on the dispersion and attenuation of the tight gas sandstone reservoirs.

Seismic Modeling and Dispersion Attribute Inversion in the Theoretical Models

In the theoretical model shown in **Figure 1**, the velocity dispersion and attenuation of the tight gas sandstone are calculated using results shown in **Figure 2**. Given a density of $2,460 \text{ kg/m}^3$ for tight sandstone, the corresponding P-wave impedance can be calculated for various gas saturations as shown in **Figure 3A**. Also, we assume that the surrounding mudstone is elastic and has a P-wave velocity of $4,000 \text{ m/s}$, a shear wave velocity of $2,350 \text{ m/s}$, and a density of $2,650 \text{ kg/m}^3$. Thus, the



frequency-independent P-wave impedance of the mudstone is shown by the gray line in **Figure 3A**.

The two intersecting points in **Figure 3A** show the frequencies where the P-wave impedance I_p of the shale equals that of the tight sandstone with a gas saturation of 0.6 and 1, respectively. Accordingly, **Figure 3B** shows that normal-incidence reflection coefficients are 0 at the two frequencies, and will change from

negative to positive for increasing frequencies across the two frequencies.

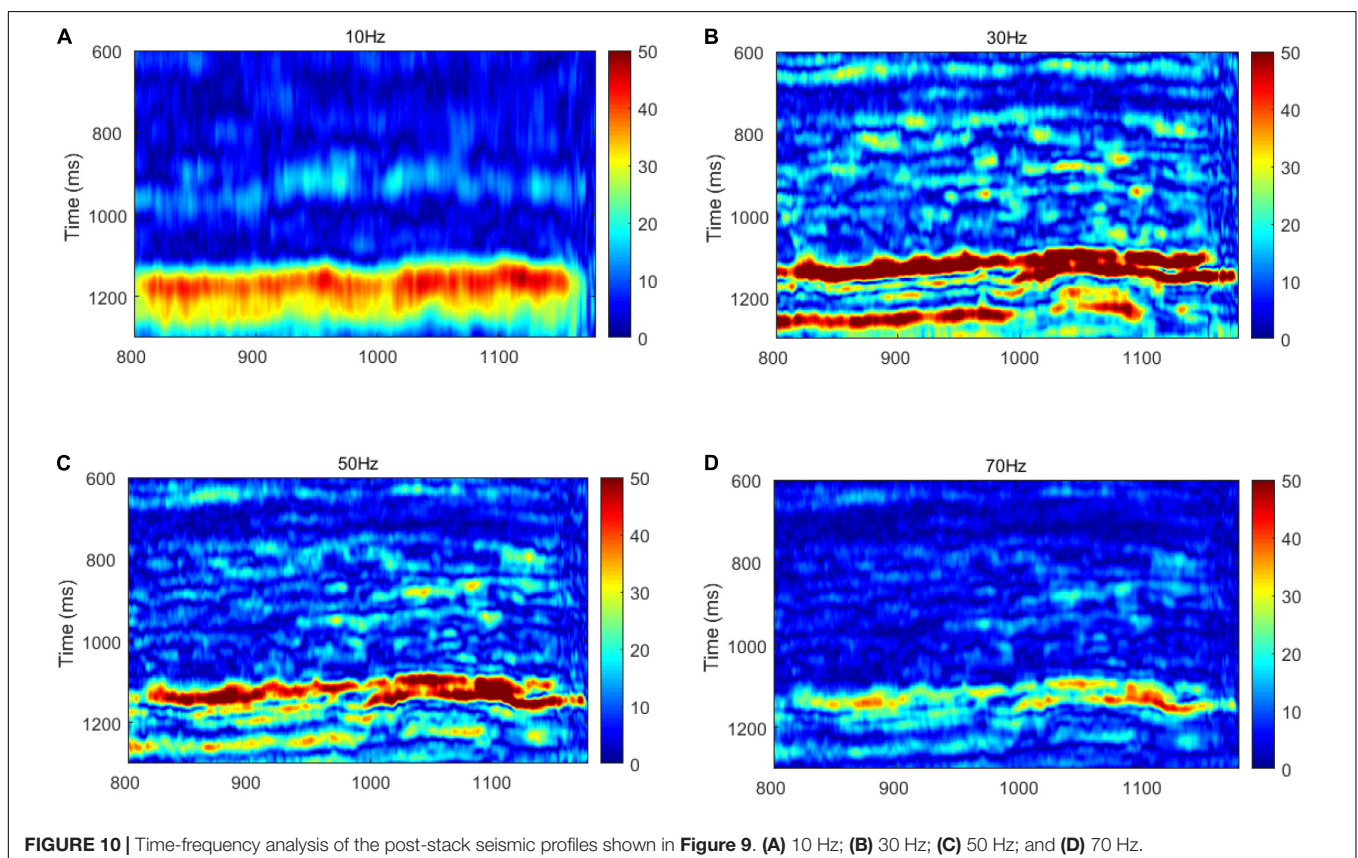
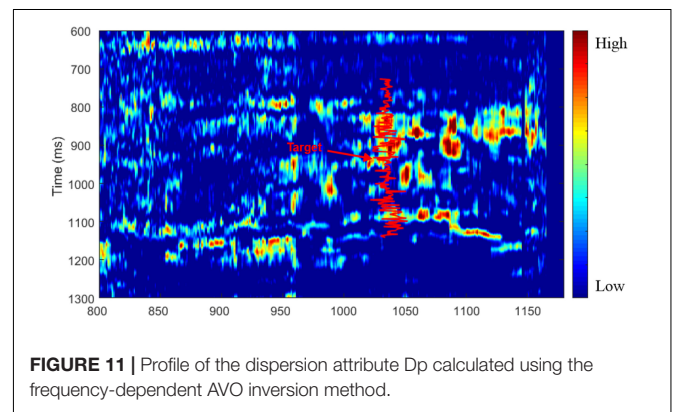
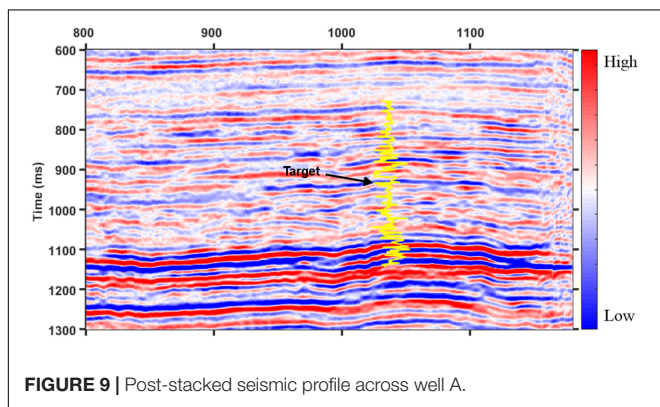
In the following, the frequency-dependent seismic responses of the tight sandstone gas reservoir are calculated using the propagator matrix method. We assume that the thickness of the tight sandstone layer is 5 m. **Figure 4** shows the absolute values of the complex frequency-dependent PP wave reflection coefficients for gas saturations of 1, 0.6, and 0, with incidence angles ranging

from 0° to 40° . For an incident Ricker wavelet of 45 Hz, the amplitude spectra of the reflected PP waves can be obtained by multiplying the spectrum of the incident Ricker wavelet by the frequency-dependent reflection coefficients. The results are shown in **Figure 5**. Furthermore, the reflected waveforms can be calculated by conducting an inverse Fourier transform of the reflected spectra. The results are shown in **Figure 6**. For the various gas saturations, there were significant differences in the PP wave frequency-dependent reflection coefficients, the spectrum, and the waveforms.

As can be seen from the AVO waveforms in **Figure 6**, the phase of the waveform for complete gas saturation is opposite

to that for complete water saturation, and the variations in the reflection amplitude with incidence angle are different. When the gas saturation is 0.6, the polarity reversal can be observed as the incidence angle increases.

Figure 7A shows the stacked seismic responses for various gas saturations obtained from AVO gathers in **Figure 6**. **Figures 7B–D** show the frequency spectrum of the AVO reflections corresponding to gas saturations of 1, 0.6, and 0, respectively. **Figure 7E** shows the P-wave dispersion attribute D_P calculated using the frequency-dependent AVO inversion method. As can be seen, the case of high gas saturation corresponds to the value of the high D_P attribute. Due to the change in reflection phase



for the case of the gas saturation of 0.6, there is a time shift for the inverted D_p attribute compared to the cases of complete gas saturation and complete water saturation. Thus, the calculation results using synthetic data of the theoretical model verify the feasibility of identifying gas-bearing tight sandstone reservoirs using the P-wave velocity dispersion attribute.

REAL DATA APPLICATIONS

Logging and Seismic Data

Figure 8 shows the logging data for the tight sandstone gas reservoir in the study area. The target layer is tight sandstone with a thickness of about 5.5 m below a depth of about 1,325 m. The target layer has a lower gamma ray value and relative higher P- and S-wave velocities than the surrounding mudstone. It has a density about 2.5 g/cm^3 and a porosity of about 0.12. The quartz content of the tight sandstone is greater than 85%.

Figure 9 shows the post-stacked seismic profile across the well. The yellow curve shows the gamma ray values from the well, and the target layer can be recognized by its low gamma value of around 920 ms.

Inversion of P-Wave Dispersion Attribute D_p

Figure 10 shows the results of the time-frequency analysis of the post-stacked seismic data in **Figure 9**. The time-frequency analysis profiles correspond to frequencies of 10, 30, 50, and 70 Hz. As shown in **Figure 10**, the variations in the strength reflected from the target layer at different frequencies form the basis for the inversion of the P-wave dispersion attributes.

Based on the frequency-dependent AVO inversion theory, the dispersion attribute profile of D_p is calculated and shown in **Figure 11**. The red curve in **Figure 11** is the logging gamma ray value. Strong P-wave velocity dispersion can be observed at the position of the target layer around 920 ms, as pointed out by an arrow.

However, in **Figure 11**, a high value of the D_p attribute can be observed just above the target zone. A reasonable interpretation on this may be the interbedded structure consisting of thin layers of mudstone and sandstone over the position of the target zone. Such interbedded layers that can be observed on logging data in **Figure 8** mean that seismic events represent more phases (peaks and troughs) as shown in **Figure 9**. Strong reflection energy reveals the presence of interference between reflected waves.

The frequency-dependent attributes of seismic reflections are affected by both the interference caused by stacked thin layers, and by the dispersion and attenuation related to fluid flow. Thus, when we intend to identify reservoir fluids using frequency-dependent attributes, it is necessary to notice this uncertainty.

When comparing **Figures 9, 11**, it is meaningful that the inverted D_p attribute reveals the location of the pay zone which has high gas saturation. Such a pay zone cannot be predicted on the post-stacked seismic profile, where the seismic events show fewer obvious variations laterally.

Figure 12 shows a horizontal slice of the RMS amplitude of the seismic reflection from the target zone. **Figure 13** is the

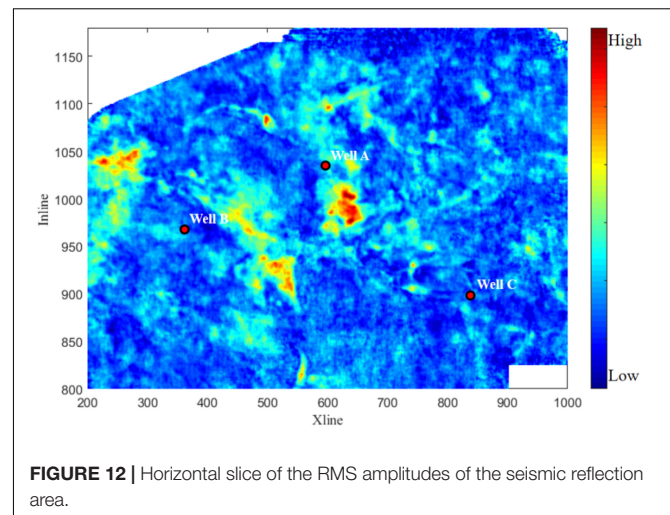


FIGURE 12 | Horizontal slice of the RMS amplitudes of the seismic reflection area.

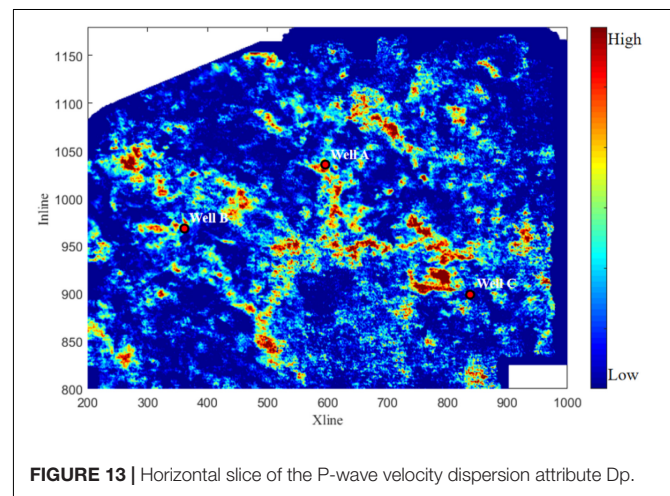


FIGURE 13 | Horizontal slice of the P-wave velocity dispersion attribute D_p .

corresponding slice of P-wave velocity dispersion attribute D_p . The values of the dispersion attribute D_p for wells A, B, and C in the study area range from high to low. The development of the reservoir shows that the productivities of the three wells are consistent with the inverted D_p attributes, which verifies the feasibility of identifying gas-bearing tight sandstone reservoirs based on frequency-dependent AVO inversion.

DISCUSSION AND CONCLUSION

We conducted rock physics modeling of tight gas sandstone by employing the Chapman theory to simulate the dispersion and attenuation caused by the squirt flow of fluids in complex pore spaces. The frequency dependence of the AVO signatures and the inversion of the P-wave dispersion attribute were investigated in different theoretical models with various gas saturations in tight gas sandstone. The field data applications of the frequency-dependent AVO inversion indicate that the estimated P-wave dispersion attribute can be used as a reliable indicator of gas identification in tight gas sandstone reservoirs.

In the constructed rock physics model, the complex pore space is equivalent to a combination of high aspect-ratio pores (stiff pores) and low aspect-ratio microcracks (soft pores). The velocity dispersion and attenuation were simulated by the squirt flow of fluids in the complex pore spaces, which is affected by the gas saturation and the viscosity of the fluid mixtures of gas and brine. The rock physics modeling revealed that as the gas saturation increases, the P-wave velocity generally decreases. P-wave velocity dispersion and attenuation occurs at seismic frequencies, and it tends to move toward higher frequencies as the gas saturation increases.

According to the rock physics modeling results, P-wave velocity dispersion in tight sandstone results in the frequency-dependence of the contrast in the elastic impedance at the interface between the tight sandstone and the overlying mudstone, and therefore, it leads to frequency-dependent reflection coefficients. The synthetic model based on the propagator matrix method revealed that the reflection coefficient varies significantly with frequency, and the variations in the amplitudes and phases of the PP reflections can be observed for various gas saturations.

The tests of the frequency-dependent AVO inversion using synthetic data revealed that the magnitude of the P-wave dispersion attribute is an effective indicator of gas saturation in the tight sandstone. Finally, the frequency-dependent AVO inversion was applied to pre-stacked field seismic data. The results indicate that the inverted P-wave dispersion attribute is

well correlated with the production of the pay zone for the evaluation wells. Thus, the methods investigated in this study have good potential for the evaluation of gas saturation in tight gas sandstone reservoirs.

DATA AVAILABILITY STATEMENT

The original contributions presented in the study are included in the article/supplementary material, further inquiries can be directed to the corresponding author.

AUTHOR CONTRIBUTIONS

ZG contributed as the corresponding author of the manuscript. HJ did a part of writing and coding works. CL, YZ, CN, DW, and YL provided some interesting ideas. All authors contributed to the article and approved the submitted version.

FUNDING

This research was supported by the China National Offshore Oil Corporation (CNOOC) research project (No. YXKY-2019-ZY-04) and the National Natural Science Foundation of China (No. 42074153).

REFERENCES

- Ba, J., Carcione, J. M., Cao, H., Du, Q. Z., Yuan, Z. Y., and Lu, M. H. (2012). Vertical wave dispersion and attenuation in unsaturated rock: wave propagation equation of dual pore medium. *Chin. J. Geophys.* 55, 219–231. doi: 10.6038/j.issn.0001-5733.2012.01.021
- Ba, J., Xu, W., Fu, L., Carcione, J. M., and Zhang, L. (2017). Rock anelasticity due to patchy-saturation and fabric heterogeneity: a double double-porosity model of wave propagation. *J. Geophys. Res. Solid Earth* 122, 1949–1976. doi: 10.1002/2016JB013882
- Ba, J., Zhao, J., Carcione, J. M., and Huang, X. (2016). Compressional wave dispersion due to rock matrix stiffening by clay squirt flow. *Geophys. Res. Lett.* 43, 6186–6195.
- Biot, M. A. (1956a). Theory of propagation of elastic waves in a fluid-saturated porous solid. I. Low frequency range. *J. Acoust. Soc. Am.* 138, 168–178. doi: 10.1121/1.1908239
- Biot, M. A. (1956b). Theory of propagation of elastic waves in a fluid-saturated porous solid. II. Higher frequency range. *J. Acoust. Soc. Am.* 138, 179–191. doi: 10.1121/1.1908241
- Carcione, J. M. (2001). AVO effects of a hydrocarbon source-rock layer. *Geophysics* 66, 419–427. doi: 10.1190/1.1444933
- Chapman, M. (2003). Frequency-dependent anisotropy due to meso-scale fractures in the presence of equant porosity. *Geophys. Prospect.* 51, 369–379. doi: 10.1046/j.1365-2478.2003.00384.x
- Chapman, M. (2009). Modeling the effect of multiple sets of mesoscale fractures in porous rock on frequency-dependent anisotropy. *Geophysics* 74, 97–103. doi: 10.1190/1.3204779
- Chapman, M., Liu, E., and Li, X. Y. (2005). The influence of abnormally high reservoir attenuation on the AVO signature. *Lead. Edge* 24, 1120–1125. doi: 10.1190/1.2135103
- Chapman, M., Liu, E., and Li, X. Y. (2006). The influence of fluid-sensitive dispersion and attenuation on AVO analysis. *Geophys. J. Int.* 167, 89–105. doi: 10.1111/j.1365-246X.2006.02919.x
- Chapman, M., Sergei, V., and Zatsepin, S. C. (2002). Derivation of a microstructural poroelastic model. *Geophys. J. Int.* 151, 427–451. doi: 10.1046/j.1365-246X.2002.01769.x
- Chen, S. Q., Chapman, M., and Wu, X. Y. (2015). The application of quantitative gas saturation estimation based on the seismic wave dispersion inversion. *J. Appl. Geophys.* 20, 81–95. doi: 10.1016/j.jappgeo.2015.07.001
- Davide, G., and Carcione, J. M. (2003). Acoustic properties of sediments saturated with gas hydrate, free gas and water. *Geophys. Prospect.* 51, 141–157. doi: 10.1046/j.1365-2478.2003.00359.x
- Dvorkin, J., and Nur, A. (1993). Dynamic poroelasticity: a unified model with the squirt and the Biot mechanisms. *Geophysics* 58, 524–533. doi: 10.1190/1.1443435
- Li, X. Y. (2013). “Quantitative estimation of gas saturation by frequency dependent AVO: numerical, physical modelling and field studies,” in *Proceedings of the 6th International Petroleum Technology Conference*, (Beijing).
- Ruiz, F., and Cheng, A. (2010). A rock physics model for tight gas sand. *Lead. Edge* 29, 1484–1489. doi: 10.1190/1.3525364
- Shuey, R. T. (1985). Simplification of the Zoeppritz equations. *Geophysics* 50, 609–614. doi: 10.1190/1.1441936
- Smith, T. M., Sayers, C. M., and Sondergeld, C. H. (2009). Rock properties in low-porosity/low-permeability sandstones. *Lead. Edge* 28, 48–59. doi: 10.1190/1.3064146
- Wang, E., Carcione, J. M., Ba, J., and Liu, Y. (2019). Reflection and transmission of plane elastic waves at an interface between two double-porosity media: effect of local fluid flow. *Surv. Geophys.* 41, 283–322.
- White, J. E. (1975). Computed seismic speeds and attenuation in rocks with partial gas saturation. *Geophysics* 40, 224–232. doi: 10.1190/1.1440520
- Wilson, A. (2010). *Theory and Methods of Frequency-Dependent AVO Inversion*. Edinburgh: The University of Edinburgh.
- Wilson, A., Chapman, M., and Li, X. Y. (2009). “Frequency-dependent AVO Inversion,” in *79th annual SEG meeting Expanded Abstracts*, Vol. 28, (Tulsa, OK: Society of Exploration Geophysicists), 341–345.
- Wood, A. W. (1995). *A Textbook of Sound*. New York, NY: The MacMillan Co, 360.

- Wu, X. Y. (2010). *Frequency Dependent AVO Inversion Using Spectral Decomposition Techniques*. Beijing: China University of Geosciences.
- Wu, X. Y., Chapman, M., Li, X. Y., and Boston, P. (2014). Quantitative gas saturation estimation by frequency-dependent amplitude-versus-offset analysis. *Geophys. Prospect.* 62, 1224–1237. doi: 10.2307/1933611
- Zhang, Z., Yin, X. Y., and Hao, Q. Y. (2014). Frequency variable fluid identification based on AVO inversion. *Chin. J. Geophys.* 12, 4171–4184. doi: 10.6038/cjg20141228

Conflict of Interest: YZ, CN, DW, and YL were employed by the company CNOOC and declare that this study received funding from CNOOC. The funder

had the following involvement with the study: YZ provided some new ideas and suggestions, CN and DW gave analysis on results, and YL collected the data.

The remaining authors declare that the research was conducted in the absence of any commercial or financial relationships that could be construed as a potential conflict of interest.

Copyright © 2021 Jin, Liu, Guo, Zhang, Niu, Wang and Ling. This is an open-access article distributed under the terms of the Creative Commons Attribution License (CC BY). The use, distribution or reproduction in other forums is permitted, provided the original author(s) and the copyright owner(s) are credited and that the original publication in this journal is cited, in accordance with accepted academic practice. No use, distribution or reproduction is permitted which does not comply with these terms.

APPENDIX A

The Frequency-Dependent AVO Theory

Shuey (1985) gave an approximate formula for the PP reflection coefficient for isotropic media:

$$R_{PP}(\theta) \approx \frac{1}{2} \left(\frac{\Delta V_P}{V_P} + \frac{\Delta \rho}{\rho} \right) + G \sin^2 \theta \quad (\text{A1})$$

where θ is the incident angle. V_P and ρ are the mean values of the P-wave velocity and density across the interface, respectively. ΔV_P and $\Delta \rho$ are the differences in the P-wave velocity and density across the interface, respectively. G is the AVO gradient.

Based on Eq. A1, Chapman et al. (2006) concluded that the dispersion of the P-wave velocity caused the frequency dependency of the reflection coefficient. Thus, Eq. A1 can be rewritten as

$$R_{PP}(\theta, f) \approx \frac{\Delta V_P}{2V_P}(f) + \frac{\Delta \rho}{2\rho} + G(f) \sin^2 \theta \quad (\text{A2})$$

Using the Taylor series expansion method, we obtained the frequency-dependent R_{PP} for a reference frequency:

$$\begin{aligned} R_{PP}(\theta, f) \approx & \frac{\Delta V_P}{2V_P}(f_0) + (f - f_0) \frac{\partial}{\partial f} \left(\frac{\Delta V_P(f)}{2V_P(f)} \right) + \frac{\Delta \rho}{2\rho} + \\ & G(f_0) \sin^2 \theta + (f - f_0) \frac{\partial G(f)}{\partial f} \sin^2 \theta \end{aligned} \quad (\text{A3})$$

Thus,

$$R_{PP}(\theta, f) = R_{PP}(\theta, f_0) + D_P(f - f_0) + D_G(f - f_0) \sin^2 \theta \quad (\text{A4})$$

where D_P represents the derivatives of the seismic wave velocities with frequency; and D_G is the frequency-dependent AVO gradient.

$$D_P = \frac{\partial}{\partial f} \left(\frac{\Delta V_P(f)}{2V_P(f)} \right), \text{ and } D_G = \frac{\partial G(f)}{\partial f} \quad (\text{A5})$$

In the application of the frequency-dependent AVO method to real data, the time-frequency spectra $S(t, \theta, f)$ of the pre-stacked gathers contains the information for the incidence wavelet spectrum, so it is necessary to eliminate the effect of the incidence wavelet.

$$M(t, \theta, f) = S(t, \theta, f) w(f, \theta) \quad (\text{A6})$$

$$w(f, \theta) = \frac{\max(A_{f=ref}(\theta))}{\max(A_f(\theta))} \quad (\text{A7})$$

where $\max(A_{f=ref}(\theta))$ is the maximum value of the amplitude spectrum in the selected time window used for the calculation.

According to Eq. A4,

$$\Delta M(t, \theta, f) = (f - f_0) (D_P + D_G \sin^2 \theta) \quad (\text{A8})$$

where $\Delta M(t, \theta, f) = M(t, \theta, f) - M(t, \theta, f_0)$.

Eq. A8 can be rewritten in the form of a matrix:

$$\begin{bmatrix} \Delta M(t, \theta_1, f_1) \\ \vdots \\ \Delta M(t, \theta_n, f_m) \end{bmatrix} = \begin{bmatrix} f_1 - f_0 & (f_1 - f_0) \sin^2(t, \theta_1) \\ \vdots & \vdots \\ f_m - f_0 & (f_m - f_0) \sin^2(t, \theta_n) \end{bmatrix} \times \begin{bmatrix} D_P \\ D_G \end{bmatrix} \quad (\text{A9})$$

where the D_P and D_G values of inversion parameters can be obtained by solving the over-determined equation.